Feeding biomechanics in the Great Barracuda during ontogeny

M. L. Habegger[1], P. J. Motta[1], D. R. Huber[2] & S. M. Deban[1]

1 Department of Integrative Biology, University of South Florida, Tampa, FL, USA
2 Department of Biology, University of Tampa, Tampa, FL, USA

Abstract

In this study we investigated bite force and functional morphology of the feeding mechanism of the great barracuda *Sphyraena barracuda* through ontogeny. Theoretical estimates of bite force at two bite points were calculated for a size series of barracuda ranging from 18 to 130 cm TL ($n = 27$) using a three-dimensional static equilibrium model. In addition, electromyography was used to determine the role of the adductor mandibulae subdivisions (A1, A2, A3) in jaw closure. All recorded subdivisions were active during jaw adduction, although onset times and activity durations differed among them. Bite force ranged from 1 to 93 N at the most anterior bite point, and from 3 to 258 N at the most posterior bite point. Mechanical advantage, in lever and posterior out lever, as well as the cross-sectional area of the majority of the adductor mandibulae subdivisions scaled with isometry; consequently bite force at both bite points also scaled with isometry. Bite force in *S. barracuda* increased in proportion to total length during ontogeny, which may be associated with a piscivorous diet throughout its life. When compared to other fishes, values of bite force in *S. barracuda* are among the lowest relative to its body size.

Introduction

Numerous factors affect resource utilization such as competition, energy consumption, risk of predation, prey availability and predator performance (Wainwright, 1991). Predator performance includes the ability of a predator to locate, capture and handle prey, all of which are influenced by morphology (Wainwright, 1988, 1991). Consequently, feeding performance is a determinant of fitness as survival is contingent upon food acquisition, and feeding performance has also been shown to affect patterns of resource use in fishes and other vertebrates (Wainwright, 1988; Hernandez & Motta, 1997; Mcbrayer, 2004; Huber et al., 2005; Herrel & O'Reilly, 2006). Ontogenetic dietary shifts are common in fishes and other vertebrates (e.g. Hernandez & Motta, 1997; Ebert, 2002; Herrel & O'Reilly, 2006) which may be explained by changes in habitat or driven by changes in predator morphology and performance over ontogeny (Wainwright & Richard, 1995; Herrel & O'Reilly, 2006; Kolmann & Huber, 2009). Identifying the causal mechanisms of these dietary shifts is key to understanding the relationship between morphology, performance and ecology in vertebrate feeding.

Among various performance measures, bite force may be one of the most important due to its ecological implications and evolutionary significance affecting organismal fitness (Herrel & Gibb, 2006; Anderson, McBrayer & Herrel, 2008).

For example, bite force performance in catfish *Clarias gariepinus* has been shown to vary with cranial size through ontogeny, where small individuals (< 30 cm TL) that feed on hard prey exhibit a disproportionally high bite force, while larger individuals that feed on elusive prey show lower relative values (Herrel et al., 2005).

Ectotherms can grow to large adult body lengths from very small juveniles, making them a good model to quantify intraspecific scaling patterns of performance through ontogeny (Robinson & Motta, 2002; Deban & O'Reilly, 2005; Herrel & O'Reilly, 2006). Additionally, studies of feeding performance through ontogeny for top predators may offer insight into the upper limits of performance. Apex predators such as large teleosts or sharks characteristically eat large prey, and consequently are expected to exert high values of absolute bite force (Huber et al., 2009). Furthermore, several studies have shown extremely high values of bite force in numerous apex predators (Erickson, Lappin & Van Vliet, 2003; Huber, Weggelaar & Motta, 2006; Wroe et al., 2008; Huber et al., 2009). However, the question remains whether this pattern of high bite force performance is common to apex predators.

The great barracuda *Sphyraena barracuda* is an apex predator that inhabits reefs and seagrass beds in most tropical seas around the world. Maturity occurs between two and four years of age ($\sim$55–73 cm TL) for males and

females, respectively (deSylva, 1963), and *S. barracuda* can reach lengths up to 180 cm TL and exceed 45 kg (deSylva, 1963). *Sphyraena barracuda* is a lie-in-wait predator with a body morphology suited for rapid acceleration (deSylva, 1963). It uses ram feeding to capture elusive prey and possesses an elongated jaw (Fig. 1), a common characteristic of ram feeding predators (Ferry-Graham, Wainwright & Bellwood, 2001; Porter & Motta, 2004). A previous theoretical analysis of bite force in an ontogenetic series of seven individuals of *S. barracuda* (20–8200 g) estimated bite forces ranging from 0.90–73 N at the most posterior bite point (Grubich, Rice & Westneat, 2008). This study differs from the previous one in the size range of animals investigated, the utilization of a three-dimensional (3D) model for the estimation of bite force, and the number of adductor mandibulae subdivisions utilized to perform these estimations.

The goals of this study are to resolve the adductor musculature involved in biting in *S. barracuda*, analyze changes in its bite force performance throughout ontogeny using a 3D static equilibrium model, and investigate the morphological correlates associated with these functional changes.
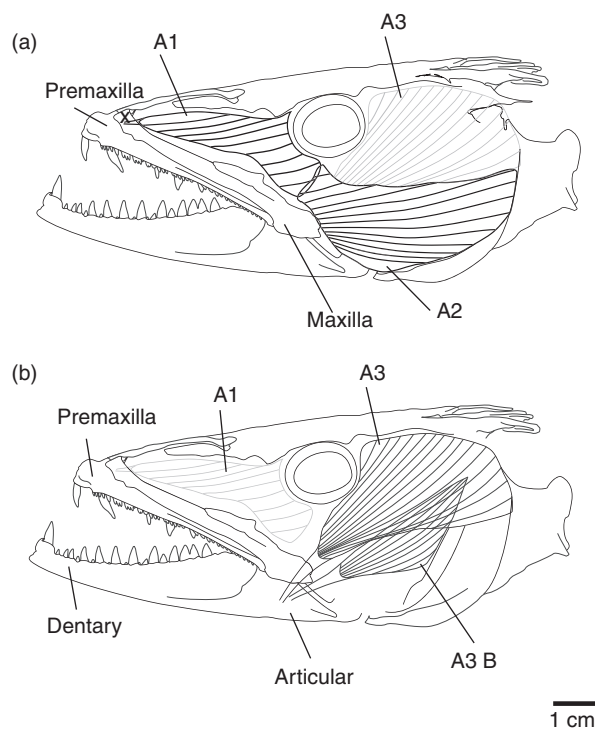
Figure 1 Lateral view of the jaw adductor muscles of *Sphyraena barracuda*. (a) Superficial subdivisions are shown. A1, adductor mandibulae subdivision 1; A2 adductor mandibulae subdivision 2; A3 adductor mandibulae subdivision 3. The 'x' denotes the area where the palatine process articulates with the maxilla (palatine is absent on the figure). (b) The deepest subdivision A3β lies deep to A2 and partially under A3.

Materials and methods

Jaw adductor activity

In order to reveal which subdivisions of the adductor mandibulae muscle are active during biting, two *S. barracuda* (20–30 cm TL) were captured in the Florida Keys and transported to the University of South Florida where they were housed together in a 380 L aquarium (salinity 32‰, temperature 20 °C). Animals were conditioned to feed on live goldfish *Carassius auratus* under bright light conditions (tungsten bulbs, 500 W) for 2–3 weeks. Prey items (3–7 cm TL) were provided at least twice a week (~25 individuals per week). Electromyographic procedures were performed following Motta, Hueter & Tricas (1991). Bipolar electrodes were prepared from strands of teflon-coated stainless steel alloy wire (0.06 mm diameter), with the end of the wires (1 mm) exposed and bent into an arrow shape to facilitate retention within the muscles. Before surgery, individuals were anesthetized with $0.1 \, \text{g L}^{-1}$ of tricaine methanesulfonate (MS-222) in a re-circulating flow tank. Bipolar electrodes were implanted in three adductor mandibulae subdivisions (A1, A2 and A3) by 26 G hypodermic needle. A total of seventeen captures were analyzed from the two individuals. In four of these captures bilateral implantation of the electrodes in the anterior subdivision, A1, resulted in up to 21 EMG bursts for this muscle. However, the other muscles and subdivisions were only unilaterally implanted. Because of technical difficulties, not all muscles and subdivisions were recorded from, resulting in some cases with <17 bursts per muscle to analyze. During the surgery, the gills were perfused with water and anesthetic. After implantation, wires were glued together with modeling cement and anchored to a surgical suture loop attached to the dorsal surface of the body, anterior to the dorsal fin. After surgery, individuals recovered in the filming tank, (the original tank subdivided into two portions resulting in a filming area of 70 × 40 cm) for at least 24 h, during which time food was not provided. After 24 h recovery period and immediately before feeding trials, wires were connected to a 16-channel AC differential amplifier (Model 3500, A-M systems, Inc, Carlsborg, WA, USA) (gain: 10000, band pass filter: 100–5000 Hz, notch filtered).

Prey items (one goldfish for each feeding event) were then introduced into the filming tank. EMG signals were captured with a data acquisition system (NI-DAQ, National Instruments, Austin, TX, USA) connected to a computer (Dell Latitude D-600). For each feeding event, EMG data capture was synchronized with high-speed digital images (Fastcam 512 PCI, Photron Inc, San Diego, CA, USA) collected simultaneously at a rate of 250 frames per second. Image data were recorded and analyzed with Photron motions tools system (Software version 1.2.0, Photron Inc, CA, USA). Electromyographic data were obtained in most feeding events from two adductor muscle divisions (A1 and A2, or A1 and A3). Only first capture bites (when prey was initially grasped between the jaws) were analyzed. In several instances, *S. barracuda* held or repositioned the prey between the jaws

before swallowing it. In these cases, data subsequent to the initial capture was not included in the analyses.

Variables analyzed for each capture event were onset time, offset time, and total duration of muscular activity for each of the adductor mandibulae subdivisions (A1, A2, A3), as well as jaw opening and jaw closing time. Jaw opening was determined as the time from the onset of jaw abduction to the time in which maximum gape was reached, jaw closing was determined as the time from the onset of mandible adduction to the time when teeth encounter the prey. Onset, offset, jaw closure and burst duration were determined relative to the time of jaw opening. All animal experimentation was performed in accordance with the Institutional Animal Care and Use Committee of the University of South Florida. (IACUC protocol # 3022 and 3241).

Feeding biomechanics

Twenty-seven specimens of *S. barracuda* (23–130 cm TL) caught in the waters off the Gulf of Mexico by local fishers were collected and kept frozen until dissection. Unilateral dissections were performed and subdivisions of the adductor mandibulae complex identified following Winterbottom (1974). After identification, each major subdivision (except for A1 and Aw not included due to their small size and low angle of insertion) was removed and bisected through its center of mass, perpendicular to the main fiber direction (all bisected muscles were parallel-fibered). Center of mass was found from the intersection of two lines estimated by suspending each muscle from a weighted line. Anatomical cross-sectional area (CSA) was traced from digital pictures (Canon Power shot A710is) using SIGMA SCAN PRO version 4 (SYSTAT Software Inc, Point Richmond, CA, USA). Theoretical maximum tetanic force (Po) for each subdivision was determined by multiplying the CSA by the specific tension of fish muscle (TS) (20 N cm^{-2}, Altringham & Johnston, 1982) following Powell *et al.* (1984).

$$P_O = CSA \times TS$$

As muscles were dissected from the skulls, 3D coordinates of origin and insertion of each adductor subdivision, jaw joint, and two bite points along the lower jaw (most proximal point, and most distal bite points) were obtained for each individual (jaws completely adducted) using a 3D digitizer (PATRIOT^{TM} digitizer, Polhemus, Colchester, VT, USA). From these points in-lever and out-lever distances were calculated. Mechanical advantage was then calculated from the ratio of the weighted in lever (based on the amount of force produced by each muscle) to the out lever. 3D force vectors were made for each subdivision of the adductor mandibulae complex that inserts on the lower jaw using P_O and the 3D position for each muscle. Theoretical maximum bite forces produced along the lower jaw were calculated via summation of moments about the jaw joint with a 3D static equilibrium model in MATHCAD 13 (Mathsoft Inc, Cambridge, MA, USA), following Huber *et al.* (2005):

$$F_{LJ} = F_{JR} + F_{A2} + F_{A3} + F_{A3\beta} + F_B = 0$$

where F_{LJ} are the forces acting on the lower jaw, F_{JR} is the jaw joint reaction force, F_{A2}, F_{A3} and $F_{A3\beta}$ are the forces generated by each adductive muscle subdivision and F_B is the bite reaction force from the prey item (Huber, 2006).

The majority of the variables (anterior and posterior bite force, weighted in lever, anterior and posterior out lever, CSA) were log-transformed and linearly regressed using least-squares regression against log total length. This type of regression was selected based on the differences of the errors from the dependent and independent variables; we expect the dependent variables to have higher error than the independent because they were estimated with a more complex approach (see methods of Robinson & Motta, 2002). Mechanical advantage was not transformed because ratios demonstrate linear behavior. For all the adductor mandibulae subdivisions the calculated force vectors were broken into their 3D components and the '*y*' component analyzed separately (note that all bite forces were calculated using fully 3D force vectors). The '*y*' component is most perpendicular to the lower jaw and therefore contributes the greatest amount to bite force generation (Kolmann & Huber, 2009). To determine scaling patterns, slopes for each regression were compared with expected isometric slopes (muscle CSA, '*y*' components of force vectors, bite forces = 2, mechanical advantage = 0, lever distances = 1). Slopes were compared by using a two-tailed student *t*-test (Sokal & Rohlf, 1995). Finally, two forward stepwise regressions were performed to determine which mechanical variables best predict anterior and posterior bite force.

Comparisons of bite force among fishes

The value of anterior bite force of the heaviest available specimen of *S. barracuda* (122 cm TL, 11 900 g) was compared with the maximum values of anterior bite force of 18 other fishes from the literature, in which variables such as bite force and mass were available (Hernandez & Motta, 1997; Clifton & Motta, 1998; Huber & Motta, 2004; Korff & Wainwright, 2004; Huber *et al.*, 2005, 2006; Huber, 2006; Huber, Dean & Summers, 2008; D. R. Huber & K. R. Mara, unpubl. data). To remove the effect of mass, values of anterior bite force were log-transformed and linearly regressed against log-transformed mass, and the residuals compared. All regressions were performed in SIGMASTAT 2.03 (SYSTAT Software Inc.).

Results

Anatomy

The adductor mandibulae of *S. barracuda* is composed of four subdivisions: A1, A2, A3 and A3β (nomenclature is based on Winterbottom, 1974) (Fig. 1). The most anterior subdivision, A1, originates on the lacrymal and part of the other infraorbitals and has a tendinous insertion on the maxilla posteroventral to its articulation with the palatine. The ventrolateral subdivision in the cheek, A2, originates along the posterior edge of the preoperculum and the

anterior margin of the operculum and inserts on the coronoid process of the articular. The largest and most robust subdivision A3 occupies the majority of the middorsal region of the cheek. It originates on the hyomandibula, preoperculum, operculum and sphenotic bones and inserts on the dentary over a notch in the Meckelian fossa by a thick tendon. Deeper to A2 and A3 lies the more medial subdivision, A3β, which originates in the anteromedial portion of the preoperculum and hyomandibula and also has a tendinous insertion in the Meckelian fossa of the dentary, dorsal to the insertion of A3. Winterbottom (1974) suggested a different nomenclature for this subdivision (Aw instead of A3β), however, the connection between A3β and Aw described by the author is not present in *S. barracuda*, suggesting A3β is a separate subdivision. The last subdivision of the adductor mandibulae complex, Aw is a small subdivision that lies along the internal margin of the dentary. Originating by a tendon on the preopercle it inserts on the dentary. Most of these muscle subdivisions have paralleled fibers except for A1 in which pinnate fibers were observed.

Prey capture and muscle activity

At the onset of a feeding event, *S. barracuda* would first orient towards the prey and then rapidly accelerated towards it after an S fast-start. *Sphyraena barracuda* ram captured small goldfish (∼3 cm TL) with an open mouth, engulfing the prey entirely and swallowing it in one bite. Large prey (5–7 cm TL) were also ram captured, but multiple processing bites were required to reposition the prey from the anterior portion of the jaw to the most posterior teeth. Occasionally, lateral head shakes accompanied by biting were used to reduce the larger prey into smaller pieces. Additionally, when the gape reached its maximum angle,

elevation of the anterior portion of the premaxilla was observed. This mechanism and its possible implications are discussed below.

A total of 17 captures were analyzed from two individuals of *S. barracuda*. All implanted subdivisions of the adductor mandibulae (A1, A2 and A3) were active during jaw adduction. Subdivision A1 was activated first, 33.5 ± 4 ms; mean $\pm$ SE after the onset of mandible depression with a mean burst duration of 89 ± 7 ms (21 bursts, eight from bilateral activity, $n = 2$). The dorsal subdivision A3 was activated second, 36.7 ± 3 ms after mandibular depression and almost immediately after the onset of A1. A3 had the shortest burst duration of the three subdivisions (44.7 ± 6 ms, 7 bursts, $n = 2$). Subdivision A2 was activated 45.4 ± 6.6 ms after jaw opening, with a mean burst duration of 99 ± 1 ms (12 bursts, $n = 2$). Jaw adduction began 62.3 ± 5 ms after onset of mandible depression (16 bites, $n = 2$) (Fig. 2).

Scaling patterns of feeding biomechanics

The CSA of subdivisions A2 and A3β scaled isometrically, while that of A3 scaled with negative allometry (slopes = 2.2, 1.9, 1.9, respectively). Although subdivision A3 produced the largest amount of force throughout ontogeny in *S. barracuda*, (Table 1, Fig. 3), the '*y*' component of the A3 force vector (perpendicular to the lower jaw) scaled isometrically (Table 1). The percentage of the force contributed from each subdivision of the adductor mandibulae complex was 63.7 (A3), 20.6 (A2) and 15.7% (A3β).

Weighted in lever and posterior out lever scaled with isometry (Table 1, Fig. 3). However, the anterior out lever scaled with negative allometry indicating that the lower jaw decreases in relative length during ontogeny (Table 1, Fig. 3). Despite negative allometry of the anterior out lever, mechanical advantage scaled with isometry for the anterior
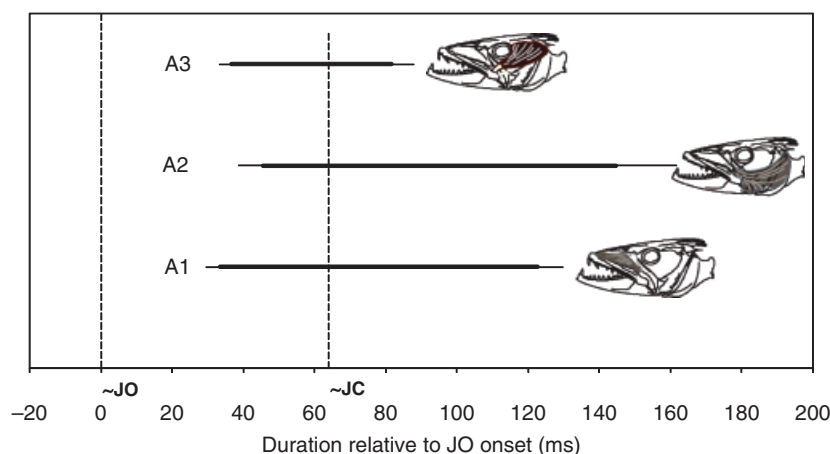

Figure 2 Composite diagram for the muscular activity of *Sphyraena barracuda* during jaw adduction. Thick horizontal bars indicate the length of activity of the different subdivisions of the adductor mandibulae; left error bars indicate 1 SE of the onset of the motor activity relative to JO; right error bars indicate 1 SE of the duration of the motor activity for each subdivision. Onset time for each subdivision is relative to the jaw opening time (JO) in ms. Jaw closing time (JC) is also relative to JO time and is defined as the time from the onset of mandible adduction to when the teeth encounter the prey.

Table 1 Results obtained from linear regressions of bite force and all variables involved with bite force in *Sphyraena barracuda*

Variable	Regression equation	Isometric slope	r^2	$t_{(0.05(2)25)}$	*P*-value
Anterior bite force (N)	Log ABF = 2.16 log TL−2.65	2	0.96	1.88	0.07
Posterior bite force (N)	Log PBF = 2.18 log TL−2.30	2	0.96	1.99	0.06
Anterior mechanical advantage	Log AMA = 0.00 log TL−0.19	0	0.12	0	1
Posterior mechanical advantage	Log PMA = 0.00 log TL−0.42	0	0.17	0	1
In lever (cm)	Log IL = 1.02 log TL−1.52	1	0.95	0.42	0.68
Anterior out lever (cm)	Log AOL = 0.95 log TL−0.73	1	0.99	3.84[a]	0.00
Posterior out lever (cm)	Log POL = 0.94 log TL−1.07	1	0.96	1.48	0.15
Cross sectional area A2	Log CSA A2 = 2.17 log TL−4.19	2	0.95	1.76	0.09
Cross sectional area A3	Log CSA A3 = 1.88 log TL−3.14	2	0.98	2.39[a]	0.02
Cross sectional area A3β	Log CSA A3β = 1.94 log TL−2.16	2	0.95	0.69	0.50
Force Vector A2 (Y-coordinate)	Log FV A2 = 2.79 log TL−5.07	2	0.58	1.66	0.11
Force Vector A3 (Y-coordinate)	Log FV A3 = 1.94 log TL−2.16	2	0.95	0.07	0.95
Force Vector A3β (*Y*-coordinate)	Log FV A3β = 2.45 log TL−3.95	2	0.80	1.83	0.08

The Y vector, which is the largest force component for each muscle, is separately regressed against TL and compared with an isometric slope.
Slopes from the regression equation were compared to isometric slopes by using a two-tail Student *t*-test.
[a]Significant deviation from geometrical similarity.
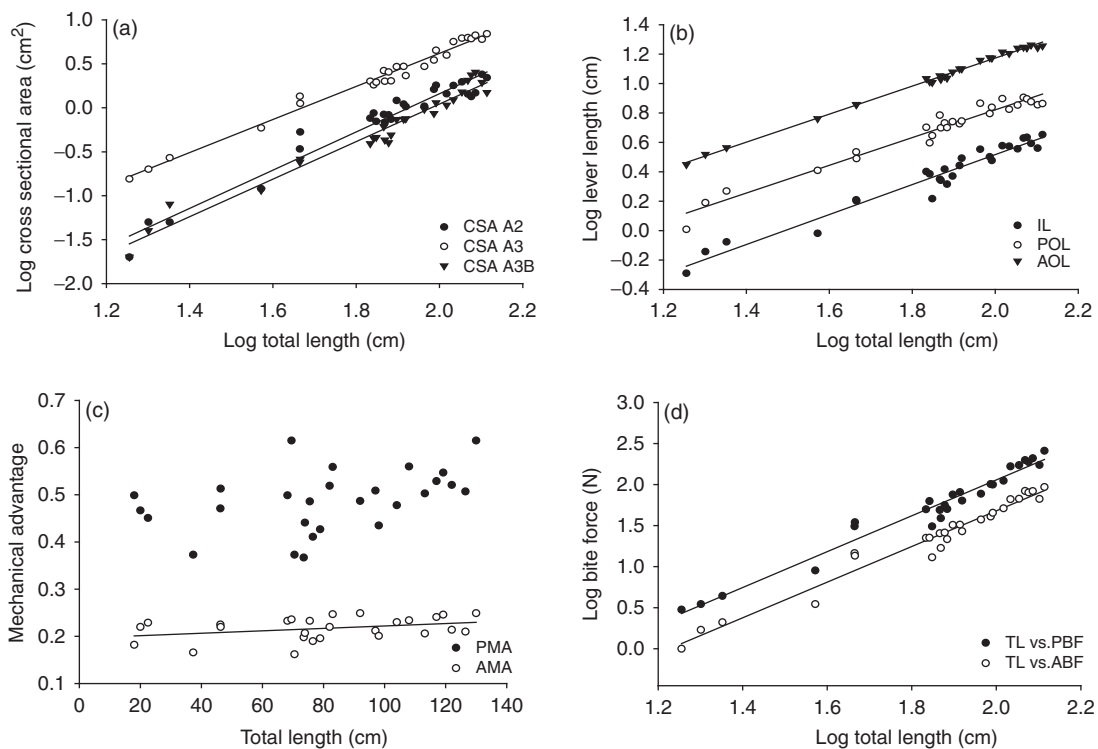
Figure 3 Variables that contribute to bite force in *Sphyraena barracuda* regressed against total length. (a) log-transformed values of cross-sectional area (CSA) of the adductor mandibulae muscle divisions regressed against log-transformed values of total length. Black circles represent values of CSA of A2 subdivision, white circles represent values of CSA of A3 subdivision and triangles represent values of CSA of A3β subdivision. (b) log-transformed values of lever lengths linearly regressed against log-transformed values of total length. Black circles represent values of in-lever distances, white circles represent values of out-lever distances at the most posterior tooth (POL) and black triangles represent values of out-lever distances at the most anterior tooth (AOL). (c) Values of mechanical advantage regressed against values of total length. Black circles represent values of mechanical advantage at the most posterior tooth (PMA), and white circles represent values of mechanical advantage at the most anterior tooth (AMA). (d) log-transformed values of bite force in *S. barracuda* regressed against log-transformed values of total length. Black circles represent posterior bite force values (PBF) and white circles represent values of bite force at the most anterior tooth (ABF). Regression lines were plotted only for significant regressions.

Table 2 Absolute values of bite force in 27 individuals of *S. barracuda*

TL (cm)	ABF (N)	PBF (N)
18	1	3
20	1.7	3.5
22.5	2.1	4.4
37.3	3.5	9
46.2	14.6	31.1
46.3	13.6	34.8
68.2	22.4	50
69.5	22.5	62.9
70.5	13	31
73.5	25.5	49
73.9	16.9	39
75.5	26	56.2
76.5	21.6	50.4
78.9	32.3	75.7
82	32.5	80.9
83	27	63.8
92	37.5	77.4
97	32.5	80.7
98.1	45.3	100
104	51.4	111.5
108	66.5	166.8
113.2	67.2	172.3
117	83.6	199
119.2	80.2	188.4
122	83.4	209.1
126.5	66.95	173.7
130	93.43	258.5

Total length (TL) expressed in cm, anterior values of bite force (ABF) and posterior values of bite force (PBF) expressed in Newtons (N).

and posterior bite points on the lower jaw (ranging from 0.18 to 0.25 and from 0.37 to 0.62, respectively) (Table 1, Fig. 3). Theoretical bite force ranged from 1 to 93 N at the anterior bite point, and from 3 to 258 N at the posterior bite point over an ontogenetic size range from 18 to 130 cm TL (Table 2), and both anterior and posterior bite force scaled isometrically (Table 2, Fig. 3). Results from the multiple regression analyses indicate that PBF can be predicted by the CSA of the adductor mandibulae subdivisions A2 and A3 ($P = 0.02$ and 0.001, regression coefficient (rc) = 0.17 and 0.85, respectively), PMA ($P = 0.03$, rc = -18.7) and in-lever length ($P = 0.02$, rc = 19.7), as well as POL ($P = 0.02$, rc = -19.9). However, ABF was best predicted by the CSA of the adductor mandibulae subdivisions A2 and A3 ($P = 0.05$ and <0.001, rc = 0.2 and 0.9, respectively).

Comparisons of bite force among fish

There was a significant relationship between the absolute values of bite force and mass among the compared species ($\log \text{ABF} = 0.272 + (0.537 \times \log \text{Mass})$, $r^2 = 0.6$ and $P < 0.001$). Absolute values of bite force in the great barracuda were greater than various shark species and all wrasses for which data are available. However, the mass-specific bite

force in *S. barracuda* was the fourth lowest among the 19 species compared (Table 3).

Discussion

Bite force in *S. barracuda* (18–130 cm TL) increased with isometry over ontogeny. These results are supported by the isometric growth patterns found in most of the variables that influence bite force (mechanical advantage, CSA of adductive muscles and lever arms). Although, the A3 sub-division of the adductor mandibulae showed negative allo-metry of CSA, the vertical components of all three subdivisions' force vectors scaled isometrically. Because the vertical component is the greatest determinant of bite force, the apparent reduction in CSA of A3 relative to total length had no effect on the overall scaling pattern of bite force (Table 1). Although mechanical advantage (anterior and posterior) scaled isometrically during ontogeny, negative allometry was found for the anterior out lever indicating a relative decrease in length of the lower jaw through onto-geny (measured to the most anterior lower tooth in *S. barracuda* which lies anterior to the upper jaw marginal teeth and does not appear to shift its relative position with ontogeny). Results from multiple linear regressions showed that PBF can be predicted by all the variables that con-tribute to bite force: CSA of two largest adductor mandibu-lae subdivisions, PMA and the lever distances that compose this ratio; however, ABF is best predicted by the CSA of these same subdivisions of the adductor mandibulae. One possible reason for the difference may be the variability in the relative length of the lower jaw among individuals (anterior out lever = 12 ± 0.9 cm; mean $\pm$ SE), which is great-er than that of the posterior out lever (posterior out lever mean = 5.4 ± 0.4 cm). CSA of the two largest divisions of the adductor mandibulae are also predictive of bite force in the bonnethead shark *Sphyrna tiburo* (Mara, Motta & Huber, 2009), and a similar predictive relationship between anterior and posterior bite force, muscle CSA and posterior lever ratios was also found for hammerhead sharks (Mara, 2010).

The isometric scaling pattern of bite force in *S. barracuda* differs from other studies where positive allometry in bite force is often found [e.g. sheephead *Archosargus probatoce-phalus* (Hernandez & Motta, 1997); the blacktip shark *Carcharhinus limbatus* (Huber *et al.*, 2006); the spotted ratfish *Hydrolagus colliei* (Huber *et al.*, 2008); the lizards *Anolis equestris* and *Anolis garmani* (Herrel & O'Reilly, 2006); and the American alligator *Alligator mississippiensis* (Erickson *et al.*, 2003)]. In most of these cases positive allometry was attributed to a hyperallometric pattern of the adductor musculature, to disproportionate increase in the mechanical advantage or to a combination of both (Her-nandez & Motta, 1997; Erickson *et al.*, 2003, Herrel & O'Reilly, 2006; Huber *et al.*, 2006, 2008).

Sphyraena barracuda is a piscivore predator that primar-ily preys on elusive fishes (deSylva, 1963). Small individuals (≤ 45 cm TL) prey on atherinids, gobiids and clupeids, while larger individuals (from 45–140 cm TL) switch to

Table 3 Values of anterior bite forces (ABF), mass, and size removed bite force (residuals) for 19 species of fishes obtained from the literature

Species name	Common name	ABF (N)	Mass (g)	Residuals
Etmopterus spinax[a]	Velvet belly lanternshark	1.6	349.1	−2.576
Etmopterus lucifer[a]	Black belly lanternshark	3.1	48	−1.243
Squalus acanthias[b]	Spiny dogfish	19.6	1065	−1.094
Sphyraena barracuda	Great barracuda	83	11 900	−1.017
Halichoeres bivittatus[c]	Slippery dick	5	19	−0.48
Carcharhinus leucas[d]	Bull shark	1023	140 341	−0.0942
Negaprion brevirostis[a]	Lemon shark	79	1219	−0.075
Thalassoma bifasciatum[c]	Bluehead wrasse	5	7	−0.0477
Sphyrna mokarran[d]	Great hammerhead shark	2432	580 598	−0.0137
Halichoeres garnoti[c]	Yellowhead wrasse	10	21	0.0312
Chiloscyllium plagiosum[a]	Whitespotted bamboo shark	93	1219	0.051
Halichoeres maculipinna[c]	Clown wrasse	11	18	0.175
Hydrolagus colliei[e]	Whitespotted chimaera	106	870	0.293
Heterodontus francisci[f]	Horn shark	206	2948	0.297
Carcharhinus limbatus[g]	Blacktip shark	423	22 092	0.354
Heptranchis perlo[a]	Sharpnose sevengill shark	245	1614	0.682
Archosargus probatocephalus[h]	Sheepshead	309	998	1.061
Lachnolaimus maximus[c]	Hogfish	290	209	1.671
Chilomycterus schoepfi[i]	Striped burrfish	380	180	1.945

[a]Huber (2006).
[b]Huber & Motta (2004).
[c]Clifton & Motta (1998).
[d]D. R. Huber & K. R. Mara (unpubl. data).
[e]Huber *et al.* (2008).
[f]Huber *et al.* (2005).
[g]Huber *et al.* (2006).
[h]Hernandez & Motta (1997).
[i]Korff & Wainwright (2004).

belonids, tetraodontids, hemiramphids and carangids (de-Sylva, 1963). The isometric pattern of bite force in *S. barracuda* suggests that its taxonomically shifting prey base does not present changes in the mechanical demands encountered during prey capture over ontogeny, whereas positive allometry in bite force has been frequently associated with ontogenetic changes in prey size and hardness (Wainwright, 1988; Hernandez & Motta, 1997; Meyers, Herrel & Birch, 2002; Herrel & O'Reilly, 2006). Thus, isometry of bite force is sufficient to maintain piscivory throughout the life history of *S. barracuda* (deSylva, 1963).

High bite forces do not seem necessary to occupy a position as an apex predator. For example, bite forces from a 122 cm barracuda are similar to that of a 61 cm TL lemon shark *Negaprion brevirostris* and a 71 cm TL whitespotted bamboo shark *Chiloscyllium plagiosum* (Huber, 2006), both of which primarily consume teleost fishes and crustaceans. Additionally, the mass-specific bite force of barracuda is among the lowest of the bony fishes that have been studied (Table 3). Other attributes that facilitate effective predation by *S. barracuda* may include skull shape, tooth morphology, and strike behavior.

The skull *of S. barracuda* is suited for ram feeding, exhibiting a long mandible equipped with numerous sharp teeth and lacking premaxillary protrusion. Prey capture is characterized by S fast-starts and rapid acceleration (Webb,

1984; Porter & Motta, 2004). Sharp teeth are known to facilitate penetration into soft prey by concentrating force onto a small surface area (Frazzetta, 1988). Performance tests with similarly sharp and pointed teeth from the mako shark *Isurus oxyrinchus* reveal a minimum penetration force of 5 N for some teleost prey (Whitenack & Motta, 2010). Consequently, the presence of sharp, blade-like teeth coupled with ram feeding behavior may contribute to successful prey capture and processing by *S. barracuda* in the absence of high bite forces (up to 93 N at the tips of the jaws).

Piscivorous fishes generally rely on speed efficient jaws to capture evasive prey (De Schepper, Van Wassenbergh & Adriaens, 2008). Low values of mechanical advantage of (0.27) and short jaw closing durations characterize *S. barracuda* as having an overall speed-efficient jaw closing mechanism (Westneat, 2004; De Schepper *et al.*, 2008). Mean jaw closing duration in juvenile *S. barracuda* was reported as 8.1 ms (Porter & Motta, 2004), which is quite fast and similar to other long jawed species such as the Florida gar *Lepisosteus platyrhincus* (7.3 ms) (Porter & Motta, 2004).

An interesting mechanism that has been mentioned but not yet described in *S. barracuda* is the pivoting of the premaxillary teeth during maximum gape (Gudger, 1918; Grubich *et al.*, 2008). During jaw opening, depression of the
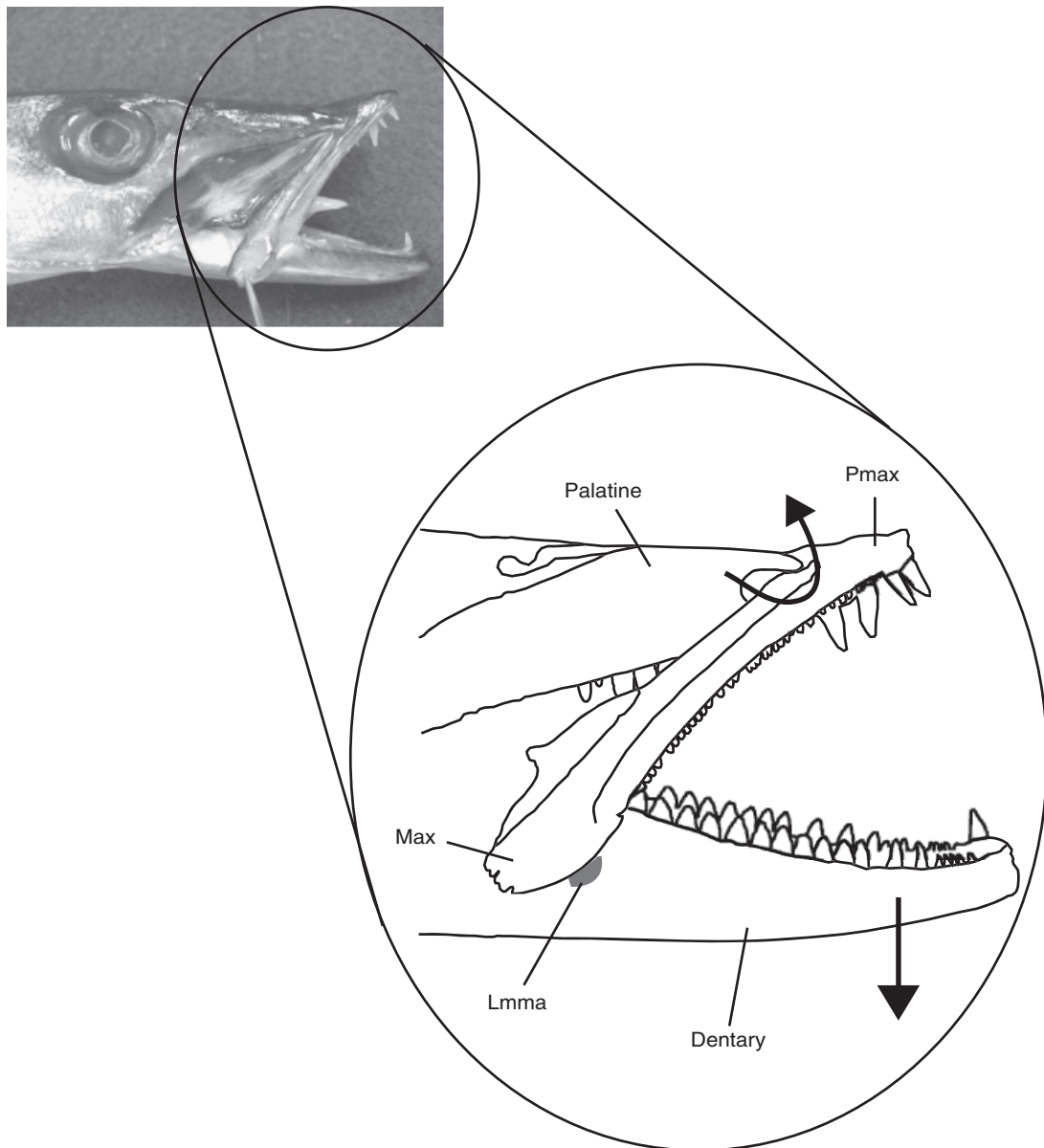
Figure 4 Premaxillary rotation during jaw opening in *Sphyraena barracuda*. Abduction of the dentary promotes the elevation of the upper jaw (maxilla and premaxilla) by the maxillomandibular ligament (Lmma). Rotation of the premaxilla occurs when the maxilla pivots around the palatine process when maximum gape size is reached. Lacrymal bone has been removed from the diagram to show the pivot point between maxilla and palatine.

dentary pulls the maxilla anteroventrally by tension in the maxillomandibular ligament. The maxilla in turn, pivots around its articulation with the anterior process of the palatine, orienting the anterior margin of the premaxilla into a more vertical position (Fig. 4). When the premaxilla swings more vertically it results in an increase in the overall anterior gape size. Larger gape size may allow predators to exploit a wider range of prey sizes not utilized by other predators, delimiting the hierarchical level occupied by a specific predator in the trophic chain (Lucifora *et al.*, 2009).

Furthermore, the rotation of the premaxilla results in a more orthogonal position of the premaxillary teeth relative to the prey, which is beneficial for prey penetration (Cundall, 2008).

Electromyographic results indicate that the adductor mandibulae subdivision 1 (A1) is an active participant during jaw adduction. This muscle inserts on the maxilla posteroventral to the pivot point with the palatine. Consequently after the prey is grasped by the fang-like teeth, A1 activates (before any other adductive musculature) rotating

the premaxilla back to its more horizontal resting position, which adducts the maxilla and closes the anterior premaxillary teeth on the prey to help prevent their escape.

Values of bite force (as well as the scaling patterns of the variables that influence it) reported in this study differ from those described by Grubich *et al.* (2008) for *S. barracuda*. Values of bite force for *S. barracuda* (25–11 900 g/ 18–130 cm TL/n = 27) in the current study ranged from 3–258 N at the most posterior bite point whereas Grubich *et al.* (2008) reported calculated values of bite force for *S. barracuda* (20–8200 g/No. TL reported/n = 7) of 0.9–73 N at the same bite positions. Differences in these results may be related to variability in the described anatomy, the use of different theoretical models (2D vs. 3D), the preservation of the specimens, or the sample size.

For example, the anatomy described by Grubich *et al.* (2008) differed in that only two subdivisions of the adductor mandibulae were included in the calculations of bite force (A2 and A3) whereas the current study includes a third subdivision (A3β), resulting in an increase in the output forces. Grubich *et al.* (2008) estimated values of bite force with a 2D model (MandibLever 3.2) (Westneat, 2004), whereas the current study used a 3D approach (Huber *et al.*, 2005). 3D models have been shown to more accurately predict bite force in mammals (Davis *et al.*, 2010). Finally, the used of preserved specimens may alter the calculations of bite force because formalin preservatives can decrease muscle mass by 8.4–13.4% in teleost fishes (Buchheister & Wilson, 2005), which may in turn affect calculated CSA, and consequently output values of bite force.

Conclusions

Sphyraena barracuda has one of the lowest relative values of bite force compared with other fishes. The scaling pattern of bite force as well as the majority of the variables that influence bite force performance increased isometrically over ontogeny. Values of mechanical advantage and jaw closing duration characterized *S. barracuda* as having an overall speed efficient jaw closing mechanism. The combination of all the results obtained from this study suggests that other strategies besides producing high bite force may contribute to the feeding success of this predator. High values of bite force are clearly not necessary for a predator to occupy an apex position in the trophic chain.

Acknowledgments

References

Altringham, J.D. & Johnston, I.A. (1982). The pCa-tension and force-velocity characteristics of skinned fibers isolated from fish fast and slow muscle. *J. Physiol.* **333**, 421–449.

Anderson, R., McBrayer, L.D. & Herrel, A. (2008). Bite force in vertebrates: opportunities and caveats for use of a nonpareil whole-animal performance measure. *Biol. J. Linn. Soc.* **93**, 709–720.

Buchheister, A. & Wilson, M.T. (2005). Shrinkage correction and length conversion equations for *Theragra chalcogramma*, *Mallotus villosus* and *Thaleichthys pacificus*. *J. Fish Biol.* **67**, 541–548.

Clifton, K.B. & Motta, P.J. (1998). Feeding morphology, diet and ecomorphological relationships among five Caribbean labrids (Teleostei, Labridae). *Copeia* **1998**, 953–966.

Cundall, D. (2008). Viper fangs: functional limitations of extreme teeth. *Physiol. Biochem. Zool.* **82**, 63–79.

Davis, J.L., Santana, S.E., Dumont, E.R. & Grosse, I.R. (2010). Predicting bite force in mammals: two-dimensional versus three-dimensional lever models. *J. Exp. Biol.* **213**, 1844–1851.

Deban, S.M. & O'Reilly, J.C. (2005). The ontogeny of feeding kinematics in the giant salamander *Cryptobranchus alleganiensis*: does current function or phylogenetic relatedness predict the scaling patterns of movement? *Zoology* **108**, 155–167.

deSylva, D.P. (1963). Systematics and life history of the great barracuda, *Sphyraena barracuda* (Walbaum). *Stud. Trop. Ocean* **1**, 1–179.

De Schepper, N., Van Wassenbergh, S. & Adriaens, D. (2008). Morphology of the jaw system in trichiurids: tradeoffs between mouth closing and biting performance. *Zool. J. Linn. Soc.* **152**, 717–736.

Ebert, D.A. (2002). Ontogenetic changes in the diet of the sevengill shark (*Notorynchus cepedianus*). *Mar. Fresh. Res.* **53**, 517–523.

Erickson, G.M., Lappin, A.K. & Van Vliet, K.A. (2003). The ontogeny of bite-force performance in American alligator (*Alligator mississippiensis*). *J. Zool. (Lond.)* **260**, 317–327.

Ferry-Graham, L.A., Wainwright, P.C. & Bellwood, D.R. (2001). Prey capture in long-jawed butterflyfishes (Chaetodontidae): the functional basis of novel feeding habits. *J. Exp. Mar. Ecol* **256**, 167–184.

Frazzetta, T.H. (1988). The mechanics of cutting and the form of shark teeth (Chondrichthyes, Elasmobranchii). *Zoomorphology* **108**, 93–107.

Grubich, J.R., Rice, A.N. & Westneat, M.W. (2008). Functional morphology of bite mechanics in the great barracuda (*Sphyraena barracuda*). *Zoology* **111**, 16–29.

Gudger, E.W. (1918). *Sphyraena barracuda; its morphology, habits, and history*. *Pap. Dept. Mar. Biol. Carnegie Inst. Wash*. **12**, 53–108.

Hernandez, L.P. & Motta, P.J. (1997). Trophic consequences of differential performance: ontogeny of oral jaw-crushing performance in the sheepshead, *Archosargus probatocephalus* (Teleostei, Sparidae). *J. Zool. (Lond.)* **243**, 737–756.

Herrel, A. & Gibb, A.C. (2006). Ontogeny of performance in vertebrates. *Physiol. Biochem. Zool*. **79**, 1–6.

Herrel, A. & O'Reilly, J.C. (2006). Ontogenetic scaling of bite force in lizards and turtles. *Physiol. Biochem. Zool*. **79**, 31–42.

Herrel, A., Van Wassenbergh, S., Wouters, S., Aerts, P. & Adriaens, D. (2005). A functional morphological approach to the scaling of the feeding system in the African catfish, *Clarias gariepinus*. *J. Exp. Biol*. **208**, 2091–2102.

Huber, D.R. (2006). *Cranial Biomechanics and Feeding Performance of Sharks*. PhD thesis, University of South Florida, Tampa, FL, USA.

Huber, D.R., Claes, J.M., Mallefet, J. & Herrel, A. (2009). Is extreme bite performance associated with extreme morphologies in sharks? *Physiol. Biochem. Zool*. **82**, 20–28.

Huber, D.R., Dean, M.N. & Summers, A.P. (2008). Hard prey, soft jaws and the ontogeny of feeding mechanics in the spotted ratfish *Hydrolagus colliei*. *J. Roy. Soc. Int*. **5**, 1–12.

Huber, D.R., Eason, T.G., Hueter, R.E. & Motta, P.J. (2005). Analysis of bite force and mechanical design of the feeding mechanism of the durophagous horn shark *Heterodontus francisci*. *J. Exp. Biol*. **208**, 3553–3571.

Huber, D.R. & Motta, P.J. (2004). Comparative analysis of methods for determining bite force in the spiny dogfish *Squalus acanthias*. *J. Exp. Zool*. **301**, 26–37.

Huber, D.R., Weggelaar, C.L. & Motta, P.J. (2006). Scaling of bite force in the blacktip shark *Carcharhinus limbatus*. *Zoology* **109**, 109–119.

Kolmann, M.A. & Huber, D.R. (2009). Scaling of feeding biomechanics in the horn shark: ontogenetic constraints on durophagy. *Zoology* **112**, 351–361.

Korff, W.L. & Wainwright, P.C. (2004). Motor pattern control for increasing crushing force in the striped burrfish (*Chilomycterus schoepfi*). *Zoology* **107**, 335–346.

Lucifora, L.O., García, V.B., Menni, R.C., Escalante, A.H. & Hozbor, N.M. (2009). Effects of body size, age and maturity stage on diet in a large shark: ecological and applied implications. *Ecol. Res*. **24**, 109–118.

Mara, K.R. (2010). *Evolution of the hammerhead cephalofoil, shape change, space utilization, feeding biomechanics in hammerhead sharks* (*Sphyrinidae*). PhD thesis, University of South Florida, Tampa, FL, USA.

Mara, K.R., Motta, P.J. & Huber, D.R. (2009). Bite force and performance in the durophagous bonnethead shark, *Sphyrna tiburo*. *J. Exp. Zool*. **311A**, 1–11.

McBrayer, L.D. (2004). The relationship between skull morphology, biting performance and foraging mode in Kalahari lacertid lizards. *Zool. J. Linn. Soc*. **140**, 403–416.

Meyers, J.J., Herrel, A. & Birch, J. (2002). Scaling of morphology, bite force, and feeding kinematics in an iguanian and a scleroglossan lizard. In *Topics in functional and ecological vertebrate morphology*: 47–62. Aerts, P., D'aout, K, Herrel, A & Van Damme, R (Eds). The Netherlands: Maastricht Shaker Publishing.

Motta, P.J., Hueter, R.E. & Tricas, T.C. (1991). An electromyographic analysis of the biting mechanism of the lemon shark, *Negaprion brevirostris*: functional and evolutionary implications. *J. Morphol*. **210**, 55–69.

Porter, H.T. & Motta, P.J. (2004). A comparison of strike and prey capture kinematics of three species of piscivorous fishes: florida gar (*Lepisosteus platyrhincus*), redfin needlefish (*Strongylura notata*), and great barracuda (*Sphyraena barracuda*). *Mar. Biol*. **145**, 989–1000.

Powell, P.L., Roy, R.R., Kanim, P., Bello, M.A. & Egerton, V.R. (1984). Predictability of skeletal muscle tension from architectural determinations in guinea pigs. *J. Appl. Physiol*. **57**, 1715–1721.

Robinson, M.P. & Motta, P.J. (2002). Patterns of growth and the effects of scale on the feeding kinematics of the nurse shark (*Ginglymostoma cirratum*). *J. Zool. (Lond.)* **256**, 449–462.

Sokal, R.R. & Rohlf, F.J. (1995). *Biometry*. New York: W. H. Freeman.

Wainwright, P.C. (1988). Morphology and ecology: the functional basis of feeding constraints in Caribbean labrid fishes. *Ecology* **69**, 635–645.

Wainwright, P.C. (1991). Ecomorphology: experimental functional anatomy for ecological problems. *Am. Zool*. **31**, 680–693.

Wainwright, P.C. & Richard, B.A. (1995). Scaling the feeding mechanism of the largemouth bass (*Micropterus salmoides*): motor pattern. *J. Exp. Biol*. **198**, 1161–1171.

Webb, P.W. (1984). Body form, locomotion and forging in aquatic vertebrates. *Am. Zool*. **24**, 107–120.

Westneat, M.W. (2004). Evolution of levers and linkages in the feeding mechanics of fishes. *Int. Comp. Biol*. **44**, 378–389.

Whitenack, L.B. & Motta, P.J. (2010). Performance of shark teeth during puncture and draw: implications for the mechanics of cutting. *Biol. J. Lin. Soc*. **100**, 271–286.

Winterbottom, R. (1974). A descriptive synonymy of the striated muscles of the Teleostei. *Proc. Acad. Nat. Sci. Phila*. **125**, 225–317.

Wroe, S., Huber, D.R., Lowry, M., McHenry, C., Moreno, K., Clausen, P., Ferrara, T.L., Cunningham, E., Dean, M.N. & Summers, A.P. (2008). Three-dimensional computer analysis of white shark jaw mechanics, how hard can a great white bite? *J. Zool*. **276**, 336–342.